


Intramuscular Near-Infrared Spectroscopy for Muscle Flap Monitoring in a Porcine Model

Wubin Bai, PhD^{1,*} Hexia Guo, MS^{2,3,*} Wei Ouyang, PhD² Yang Weng, MS² Changsheng Wu, PhD²
 Yihan Liu, MS¹ Hao Zang, PhD² Lauren Jacobson, MD⁴ Yameng Xu, MS⁵ Di Lu, PhD²
 Ziyang Hu, PhD² Shuo Li, PhD² Hany M. Arafa, MS² Quansan Yang, BS^{2,6}
 Amanda M. Westman, PhD⁴ Matthew R. MacEwan, MD, PhD⁷ John A. Rogers, PhD^{2,3,6,8,9}
 Mitchell A. Pet, MD⁴ 

¹ Department of Applied Physical Sciences, The University of North Carolina at Chapel Hill, Chapel Hill, North Carolina

² Department of Materials Science and Engineering, Querrey Simpson Institute for Bioelectronics, Northwestern University, Chicago, Illinois

³ Department of Materials Science and Engineering, Northwestern University, Evanston, Illinois

⁴ Division of Plastic and Reconstructive Surgery, Department of Surgery, School of Medicine, Washington University, St. Louis, Missouri

⁵ Department of Mechanical Engineering and Materials Science, Washington University, St. Louis, Missouri

⁶ Department of Mechanical Engineering, Northwestern University, Evanston, Illinois

Address for correspondence Mitchell A. Pet, MD, 660 S. Euclid Avenue, St. Louis, MO 63110

(e-mail: mpet@wustl.edu). John A. Rogers, PhD, 2145 Sheridan Road, Evanston, IL 60208 (e-mail: jrogers@northwestern.edu).

⁷ Department of Neurosurgery, School of Medicine, Washington University, St. Louis, Missouri

⁸ Department of Biomedical Engineering, Northwestern University, Evanston, Illinois

⁹ Department of Neurological Surgery, Feinberg School of Medicine, Northwestern University, Chicago, Illinois

J Reconstr Microsurg

Abstract

Background Current near-infrared spectroscopy (NIRS)-based systems for continuous flap monitoring are limited to flaps which carry a cutaneous paddle. As such, this useful and reliable technology has not previously been applicable to muscle-only free flaps where other modalities with substantial limitations continue to be utilized.

Methods We present the first NIRS probe which allows continuous monitoring of local tissue oxygen saturation (StO₂) directly within the substance of muscle tissue. This probe is flexible, subcentimeter in scale, waterproof, biocompatible, and is fitted with resorbable barbs which facilitate temporary autostabilization followed by easy atraumatic removal. This novel device was compared with a ViOptix T.Ox monitor in a porcine rectus abdominus myocutaneous flap model of arterial and venous occlusions. During these experiments, the T.Ox device was affixed to the skin paddle, while the novel probe was within the muscle component of the same flap.

Results The intramuscular NIRS device and skin-mounted ViOptix T.Ox devices produced very similar StO₂ tracings throughout the vascular clamping events, with obvious and parallel changes occurring upon vascular clamping and release. The normalized cross-correlation at zero lag describing correspondence between the novel intramuscular NIRS and T.Ox devices was >0.99.

Conclusion This novel intramuscular NIRS probe offers continuous monitoring of oxygen saturation within muscle flaps. This experiment demonstrates the potential suitability of this intramuscular NIRS probe for the task of muscle-only free flap monitoring, where NIRS has not previously been applicable. Testing in the clinical environment is necessary to assess durability and reliability.

Keywords

- ▶ free flap
- ▶ near-infrared spectroscopy
- ▶ perfusion monitoring

* *These authors contributed equally to this work.*

received
 May 11, 2021
 accepted
 May 31, 2021

© 2021. Thieme. All rights reserved.
 Thieme Medical Publishers, Inc.,
 333 Seventh Avenue, 18th Floor,
 New York, NY 10001, USA

DOI <https://doi.org/10.1055/s-0041-1732361>.
 ISSN 0743-684X.

Microsurgical transfer of a free muscle flap requires microvascular anastomosis to establish tissue perfusion. In the first several postoperative days, these anastomoses are susceptible to thrombosis and careful monitoring of the transferred muscle is included in the standard of care. Given the short time period after anastomotic thrombosis wherein a threatened flap may be salvageable, prompt detection of this complication is desirable.¹

Serial physical examination and external pencil Doppler check are widely employed method of muscle flap monitoring, but these intermittent modalities are limited by their inherently subjective nature and requirement for skilled bedside personnel.² Overlying dressings, skin graft, and variable lighting complicate serial visual assessment, and probe positioning and nearby nonpedicle vessels may confound external Doppler examination. Additionally, intermittent assessment strategies are subject to delayed detection of malperfusion because clear external signs of flap malperfusion may take several hours to become clinically apparent.²

Internal Doppler systems³⁻⁵ have been designed to mitigate some of the earlier concerns. These systems position a wired Doppler probe directly at (Synovis Flow Coupler⁵; Baxter Inc., Deerfield, IL) or adjacent to the anastomosis (Cook-Swartz Doppler^{3,4}; Catalent Inc., Somerset, NJ), and provide a continuous audible signal which reflects blood flow in the monitored artery or vein. While this may reduce the delay in detecting flap malperfusion associated with intermittent monitoring strategies and improve flap salvage rate,^{6,7} these systems provide subjective data that is not suited to remote monitoring, and still require frequent attendance by skilled bedside nurses to interpret the data stream. Furthermore, these systems have a high rate of false-positive alarms due to probe disengagement.⁸⁻¹¹ These events require immediate flap assessment by the surgeon, and may even result in unnecessary emergent re-exploration.¹⁰ Finally, as these wired probes are positioned directly at or adjacent to the anastomosis, they may cause deformation of or trauma to the anastomosis during placement, monitoring, and/or removal.^{5,7,8}

In flaps which carry a skin paddle, many of the above limitations have been overcome in recent years with application of near-infrared spectroscopy (NIRS) to the task of free flap monitoring. In the United States, ViOptix Inc. (Fremont, CA) is a market leader in this space, and their T.Ox device has gained wide adoption.^{7,9,12,13} This noninvasive skin-mounted peripheral monitor is capable of using backscattered near-infrared (NIR) light to measure tissue oxygen saturation (StO₂) which describes skin perfusion. This highly sensitive⁹ device provides continuous objective data, reduces the demand on bedside personnel, and facilitates remote monitoring. Also, as it is positioned peripherally, it does not pose a threat to the delicate anastomoses. Unfortunately, as currently available NIRS devices require a cutaneous skin paddle for application, this technology is not currently useful for muscle-only flap monitoring.

Recognizing the benefits of peripheral NIRS-based sensors compared with intermittent monitoring and/or centrally placed continuous Doppler devices, it was our aim to

expand the applicability of NIRS technology to include muscle flap monitoring. In this article, we introduce an intramuscular NIRS probe which measures the StO₂ of muscle flaps continuously and in real time. This probe is subcentimeter, biocompatible, flexible, waterproof, self-stabilizing, and removable. Performance of this device is evaluated in a head-to-head comparison with the T.Ox system in a porcine rectus abdominus myocutaneous flap model of arterial and venous compromise. It was our hypothesis that the intramuscular NIRS probe would generate an StO₂ tracing similar to the skin-mounted T.Ox probe throughout conditions of flap perfusion, ischemia, and congestion.

Materials and Methods

Intramuscular NIRS Probe

Fig. 1 presents schematic representations of an intramuscular NIRS probe and its operational modality. A thin narrow polymeric substrate (polyimide; thickness, 75 μm; width, 400 μm) supports a collection of thin metal traces (copper; thickness, 18 μm; width, 90 μm) that interconnect 2-micron scale, silicon-based NPN phototransistors (length, 390 μm; width, 390 μm; thickness, 185 μm). A thin encapsulation layer (parylene, thickness, 14 μm) conformally coated onto the probe prevents penetration of biofluids into the electronic components and ensures extended longevity of device performance. Arrays of thin barbs made by laser cutting a bioresorbable polymeric film (poly(lactic-co-glycolic acid) [PLGA]) extend along the edges of the probe, as anchors to fix the location of the probe at its implantation site and minimize motion relative to the surrounding tissue. These

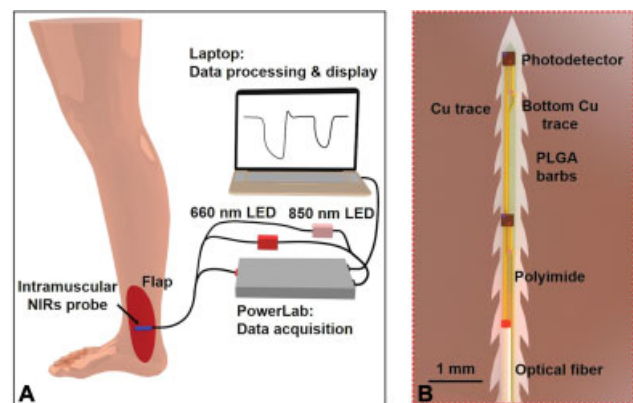


Fig. 1 An implantable intramuscular probe for providing real-time analysis of near-infrared spectroscopy (NIRS) on muscle flap. (A) Schematic illustration of the use of an implanted intramuscular NIRS probe for monitoring tissue oxygenation inside the flap muscle. The system consists of an intramuscular NIRS probe, interfaced to a data acquisition system (PowerLab, ADInstruments, Inc) for signal collection and transmission to a computer for real-time analysis and control. (B) Top-down view schematic illustration of the design of an intramuscular NIRS probe, which consists of a flexible printed circuit board, an optical fiber, sensing components (Si-based NPN phototransistors), and bioresorbable barbs. The probe is conformally encapsulated with a layer of transparent, biocompatible parylene and has a diameter of 700 μm. The barbs interface with the surrounding tissue to minimize motions and their adverse effects on signal quality.

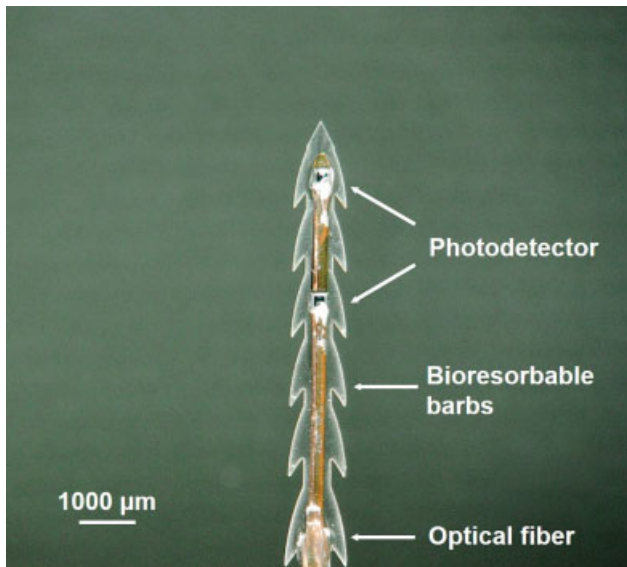


Fig. 2 Image of an intramuscular near-infrared spectroscopy probe, which highlights the sensing components (Si-based NPN phototransistors; voltage bias, 2.5 V; photocurrents generated from the phototransistors are converted into voltage signals by a transimpedance amplifier), optical fiber, and bioresorbable barbs.

PLGA barbs undergo slow hydrolysis reaction with water at the implantation site, thus can terminate their anchoring effects after a defined period of time ranging from 1 day to several weeks depending on the thickness of the barbs.¹⁴ The portion of the probe which remains after barb resorption has a needle-like shape that facilitates the device withdrawal with minimal resistance.¹⁵ A thin silica-based optical fiber (diameter, 230 μm) attached on top of the NIRS probe delivers alternating red (660 nm) and NIR (850 nm) light (frequency, 2 Hz) from external light sources (fiber-coupled LEDs, Thorlabs, Inc.) to the tip of the probe. This system offers a high degree of bendability (minimum bending curvature, 5 mm) without affecting the optoelectronic performance. The distance between the end of the optical fiber and the nearest photodetector (PD) is 5 mm, and the distance between the two PDs is 3 mm. This arrangement optimizes the signal-to-noise ratio and ensures sufficient light-tissue interactions. A data acquisition system (PowerLab, ADInstruments, Inc) captures the electrical signals in the form of voltage converted by a transimpedance amplifier from photocurrent generated by the two phototransistors. ▶**Fig. 2** shows the overall size and thin, flexible form factor of the probe and its bioresorbable barbs.

Porcine Model

Animal research was performed with the approval of the Institutional Animal Care and Use Committee at Washington University School of Medicine. This was performed as per U.S. Department of Agriculture Animal Welfare Regulations at an accredited facility. Four live pigs were utilized in separate experiments for this study. Anesthesia was induced with Telazol, ketamine, and xylazine followed by maintenance with inhaled isoflurane. After the completion

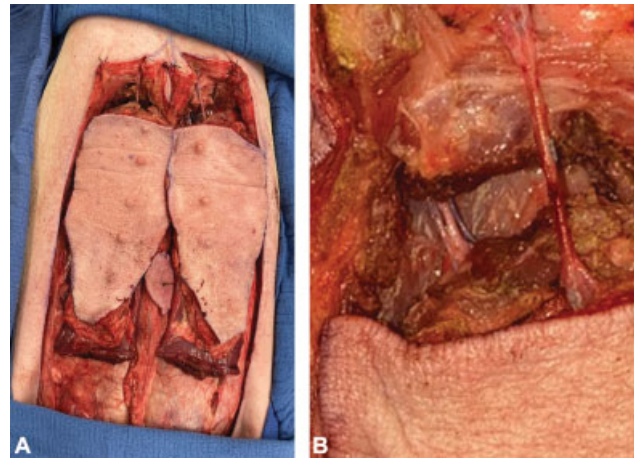


Fig. 3 (A) Bilateral pedicled rectus abdominus muscle have been raised in a live anesthetized pig. In these experiments, the left flap was used to test the intramuscular near-infrared spectroscopy device against a ViOptix T.Ox control, and the right flap was used to test other novel sensors. (B) A closer look at the deep superior epigastric artery and venae comitans, in addition to the superficial superior epigastric vein supplying the left flap.

of all experimentation, the animal was euthanized with pentobarbital.

A left pedicled rectus abdominus myocutaneous flap was raised based on the deep superior epigastric artery and veins in addition to the superficial superior epigastric vein (▶**Fig. 3**). This flap harvest procedure was adapted from Bodin et al.¹⁶

Experimental Design

To deploy the intramuscular NIRS probe, a 15 blade was used to make stab incision oriented along the axis of the muscle fibers on the undersurface of the rectus abdominus muscle, being careful to avoid the pedicle vessels (▶**Video 1**). The probe was then inserted into the muscle pocket. The entire deployment procedure took less than 30 seconds. The resorbable barbs on the probe secured its position after insertion and no additional fixation was necessary (▶**Fig. 4**). The flap was restored to its anatomic orientation and the intramuscular NIRS probe was connected to its external processor. A ViOptix T.Ox probe was adhered to the central portion of the skin paddle and then attached to the external monitor via the fiberoptic cable. Each myocutaneous flap was monitored continuously throughout the experiment using both devices in parallel (▶**Fig. 5**).

Video 1

Insertion procedure for intramuscular near-infrared probe. Online content including video sequences viewable at: <https://www.thieme-connect.com/products/ejournals/html/10.1055/s-0041-1732361>.

After achieving a stable baseline reading for each device for 15 minutes, an Acland clamp was applied to the right deep

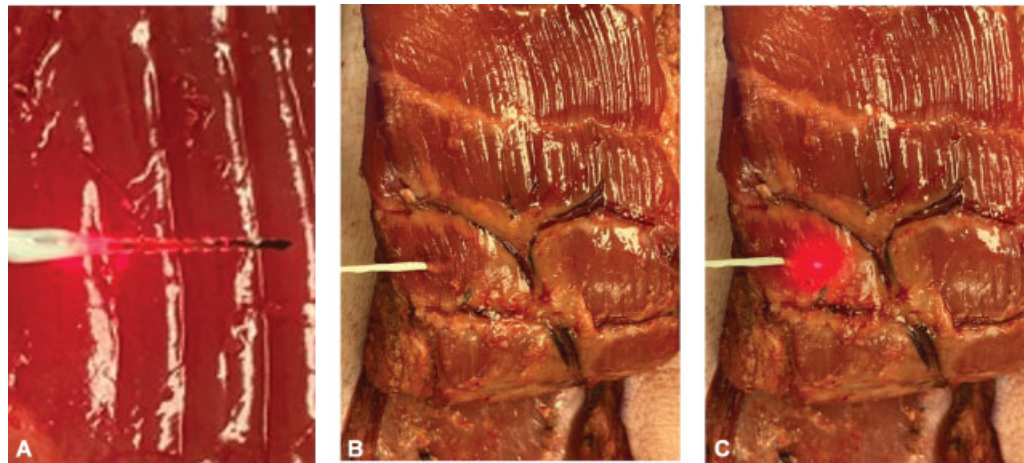


Fig. 4 The intramuscular near-infrared spectroscopy probe is shown before insertion (A). The near-infrared light is activated, and the small resorbable barbs are visible. The probe is also shown within the muscle after insertion but prior to activation (B), and after activation of the light source (C).

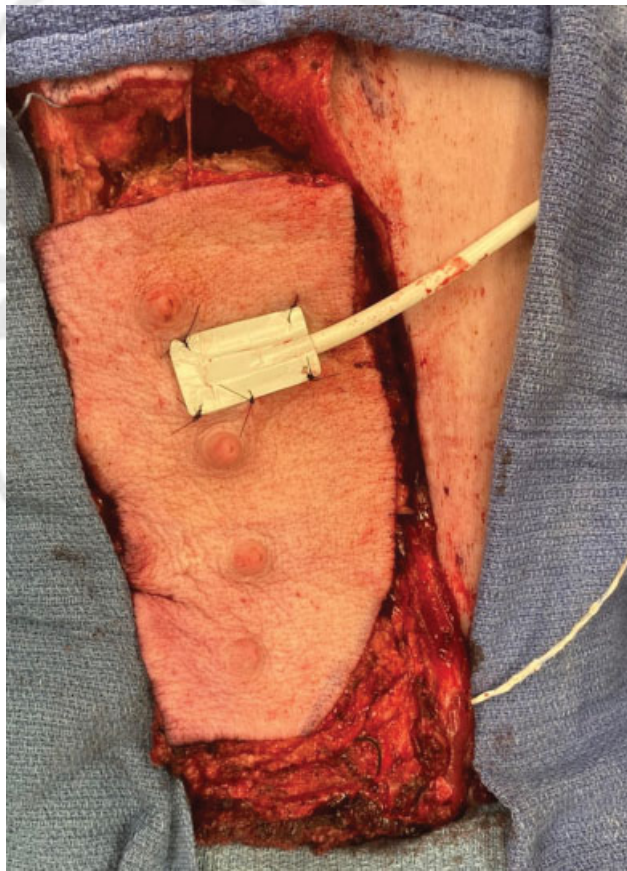


Fig. 5 The ViOptix T.Ox device is seen affixed to the skin paddle of a left rectus abdominus myocutaneous flap, and the novel intramuscular near-infrared spectroscopy probe is seen entering the underlying rectus abdominus muscle laterally.

superior epigastric artery to induce complete ischemia. Ischemia was maintained for 15 minutes. The Acland clamp was then released and 15 minutes were then allowed for flap recovery and re-establishment of a stable baseline reading. Acland clamps were then applied to the deep and superficial superior epigastric veins to induce venous congestion. Con-

gestion was maintained for 15 minutes. The Acland clamps were then released and 15 minutes were then allowed for flap recovery and re-establishment of a stable baseline reading. The entire cycle then repeated one additional time using the same flap. This experiment was then replicated twice using new probes, and separate animals on separate days to demonstrate reproducibility. A fourth experiment was done on a separate animal using two intramuscular probes deployed within the same flap (in addition to T.Ox) to demonstrate consistency between intramuscular probes.

StO₂ Calculation

Evaluation of blood saturation in the porcine model used optical densities (ODs) corresponding to red light (660 nm) and NIR light (850 nm) by converting averages of the respective signals collected by the data acquisition system based on the equation¹⁷:

$$OD(i) = -\ln(I(i)/I_0) \quad (1)$$

where $I(i)$ is the recorded signal intensity during the animal experiments and I_0 is the intensity of light emitted from the tip of the fiber. Based on measurements with a blood gas analyzer, the concentration of hemoglobin and oxygen saturation were fixed to 15 g/dl and 39%,¹⁷ respectively, for the initial phase of experiments. With the molar mass of hemoglobin (65 kg/mol), these assumptions yielded a baseline HbO_2 and Hb concentration in blood of $HbO_{20} = 0.90$ mM and $Hb_0 = 1.41$ mM, respectively. Calculation of changes in HbO_2 , ΔHbO_2 , and Hb, ΔHb exploited the modified Beer-Lambert's law¹⁷⁻¹⁹:

$$\begin{bmatrix} \Delta HbO_2(i) \\ \Delta Hb(i) \end{bmatrix} = \frac{1}{\rho_{eff}} \begin{bmatrix} \epsilon_{HbO_2R} & \hat{a}_{HbR} \\ \epsilon_{HbO_2IR} & \hat{a}_{HbIR} \end{bmatrix}^{-1} \times \begin{bmatrix} OD_R(i) \\ OD_{IR}(i) \end{bmatrix} \quad (2)$$

where ρ_{eff} is the effective photon path in the back-reflection recording geometry and ϵ are the extinction coefficients for

the two chromophores (oxygenated hemoglobin and deoxygenated hemoglobin).

The saturation of the intramuscular regime can be calculated using:

$$SO_2(i) = \frac{HbO_{20} + \Delta HbO_2(i)}{HbO_{20} + \Delta HbO_2(i) + Hb_0 + \Delta Hb(i)}$$

The effective photon path of the probe was estimated experimentally by fitting $SO_2(i)$ to the saturation values collected by the blood gas analyzer.

Statistical Methods

Each experiment yielded 2,000 to 4,000 consecutive StO_2 readings per sensor. Normalized cross-correlation at zero lag was used to describe the correspondence between the wireless NIRS and T.Ox sensors being compared.

Results

The ischemic and congested conditions were successfully achieved and recovered using the earlier protocol, as confirmed by the expected changes in flap color and StO_2 . Continuous monitoring was accomplished using both devices throughout each of the two cycles of ischemia and congestion. We encountered no technical disruptions or signal loss using either device. The intramuscular and cutaneous (T.Ox) NIRS devices produced very similar StO_2 tracings throughout the vascular clamping events, with precipitous changes occurring upon arterial clamping, arterial release, venous clamping, and venous release. The intramuscular and cutaneous NIRS tracings for the first three animal trials are shown in **Figs. 6–7** to **8**. Small interdevice variations in absolute StO_2 value readings and magnitude of change were observed. The normalized cross-correlations at zero lag describing correspondence between the intramuscular NIRS probe and T.Ox devices were

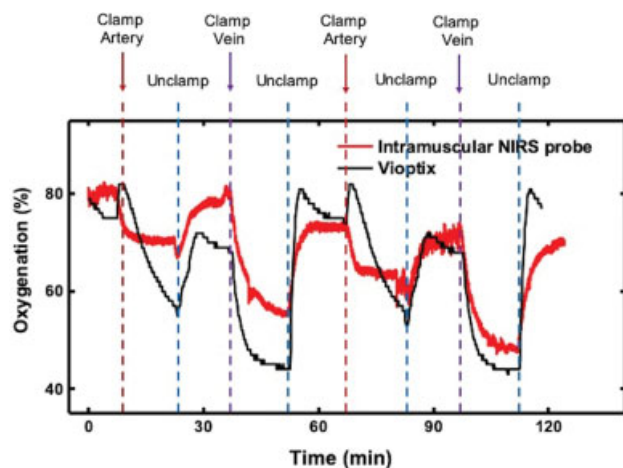


Fig. 6 Simultaneous tissue oxygen saturation traces from the intramuscular near-infrared spectroscopy (NIRS) and ViOptix T.Ox probes during conditions of flap baseline perfusion, ischemia, recovery/baseline, congestion, and recovery/baseline (two cycles in succession; Animal 1).

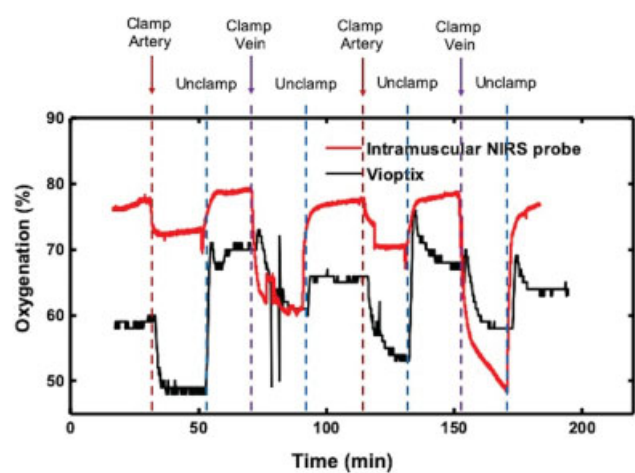


Fig. 7 Simultaneous tissue oxygen saturation traces from the intramuscular near-infrared spectroscopy (NIRS) and ViOptix T.Ox probes during conditions of flap baseline perfusion, ischemia, recovery/baseline, congestion, and recovery/baseline (two cycles in succession; Animal 2).

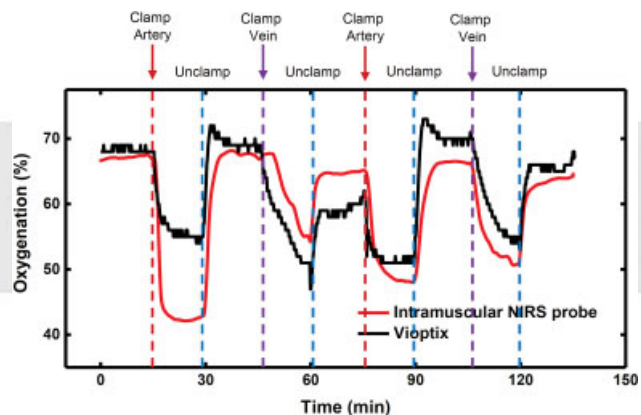


Fig. 8 Simultaneous tissue oxygen saturation traces from the intramuscular near-infrared spectroscopy (NIRS) and ViOptix T.Ox probes during conditions of flap baseline perfusion, ischemia, recovery/baseline, congestion, and recovery/baseline (two cycles in succession; Animal 3).

0.9908, 0.9934, and 0.9978, respectively, for the first three animals. For the fourth animal, two intramuscular NIRS probes were deployed into the flap for monitoring the muscular oxygenation simultaneously, in comparison with that of a T.Ox devices mounted on the flap skin (**Fig. 9**). The normalized cross-correlations at zero lag describing correspondence between the first probe and the T.Ox device, between the second probe and the T.Ox device, and between the first and the second probes are 0.9981, 0.9978, and 0.9980, respectively.

Discussion

The task of continuous free flap monitoring has been greatly facilitated by the advent of NIRS technology. However, as available devices require a cutaneous paddle to accommodate the probe, this technology has not been applicable to muscle-only flaps. In this article, we offer proof of concept for a novel intramuscular NIRS probe which mirrors the

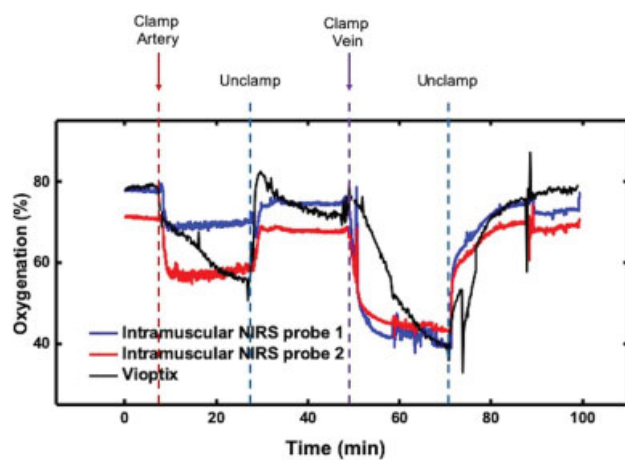


Fig. 9 Simultaneous tissue oxygen saturation traces from two separate intramuscular near-infrared spectroscopy (NIRS) probes and one ViOptix T.Ox probe during conditions of flap baseline perfusion, ischemia, recovery/baseline, congestion, and recovery/baseline (one cycle; Animal 3).

continuous monitoring functionality of the ViOptix T.Ox device, without the need for a cutaneous paddle.

Potential Advantages of the Intramuscular NIRS Probe

This strategy of intramuscular NIRS monitoring has several potential advantages compared with the implantable Doppler systems which are currently used for muscle-only free flap monitoring. First, as opposed to implantable Doppler systems which require deployment at or adjacent to the delicate vascular anastomosis, the intramuscular NIRS probe is applied peripherally within the substance of the muscle. This obviates the significant concern that the probe might kink, compress, avulse, or otherwise disrupt the anastomosis and threaten the flap.^{5,7,8} Second, while implantable Doppler systems generates auditory data which is only available at bedside, the intramuscular NIRS probe generates a continuous StO₂ tracing. This important difference reduces the care burden for bedside personnel, produces a recordable data stream, facilitates remote monitoring, and requires less subjective interpretation which makes it more robust to frequent transitions of care. Finally, while unintentional probe avulsion may affect any wired monitoring device, the peripherally inserted NIRS device could be easily replaced at bedside which implantable Doppler probes cannot. Furthermore, considering the source material and fabrication processes, a rough estimation suggests that the cost of an intramuscular NIRS probe could be as low as \$15. This is substantially less than the \$380 to 1,450 price of Cook Doppler, flow coupler, and T.Ox probes.⁷

Intramuscular NIRS Probe Design

This novel device includes two PDs mounted at increasing distances beyond a light source at the end of an optical fiber. The light enters the volume of muscle surrounding it, and the PDs record the intensity of backscatter at each of two wavelengths. These data are transmitted via wired connection to an external console and local muscle StO₂ is calculated in real time based on the known differential absorptive properties of oxygenated and deoxygenated hemoglobin.

The optical fiber is very flexible, and the probe at its tip is subcentimeter in scale. The entire assembly is encased in waterproof and biocompatible polymer layer. Probe deployment requires only a single muscular stab incision in a location remote from visible vessels. Early iterations of this device required suture fixation to maintain stable placement, but this need has been eliminated by the addition of barbs on the probe which slide into the muscle easily, but will not slide out. The barbs are made from polyglactin, which is the same resorbable polymer which comprises Vicryl suture, and are designed to maintain probe stability during use before harmlessly dissolving prior to removal by gentle traction on the fiber.

Proof-of-Concept Experimentation

It was our hypothesis that the intramuscular NIRS probe would produce a similar StO₂ tracing as a skin mounted T.Ox probe throughout conditions of perfusion, ischemia, and congestion. This hypothesis was tested using a myocutaneous flap model that allowed us to mount both sensors on the same flap, thereby producing parallel and comparable StO₂ tracings. We found that both the skin mounted and intramuscular probes detected immediate and precipitous drops in the StO₂ tracing upon arterial or venous occlusion and prompt increases upon release of the clamps. Cross-correlation values (using the >20,000 StO₂ data points gathered over the course of experimentation in four animals) between the two devices were >0.99, indicating strict agreement between the two sensors tested at all times.

Small interdevice variations in absolute StO₂ value and magnitude of change were observed. This is expected given that muscle and skin have different metabolic rates, and may have different levels of baseline and perturbed oxygen saturation. Despite these minor variations, we believe that the cutaneous or intramuscular NIRS StO₂ curve alone would have been interpreted identically in a clinical setting. In the third animal, there was again very close correspondence between both muscle probes, and between each muscle probe and the cutaneous comparator. Small differences between the two simultaneous muscle probe measurements are attributable to local oxygenation gradients within the muscle.

Study Limitations and Future Work

While this study introduces proof of concept for a new technology with direct applicability to an unmet clinical need, it has several limitations. This nonsurvival animal model does not simulate all the demands of the postmicrosurgical clinical environment. Clinical situations of microvascular compromise may be more complex than the complete and instantaneous vascular occlusive events simulated in our model, and real-world clinical testing will be necessary to validate the clinical utility and safety of this new tool. Without human clinical testing, no conclusions regarding the sensitivity and/or specificity of this device can be drawn. However, given that in-human testing must necessarily be preceded by a demonstration of device efficacy in an animal model, this study represented a necessary preclinical step in the maturation of this technology.

The nonsurvival nature of our animal protocol prohibited the necessary study of barb dissolution and probe durability over time. As such, probe longevity and stability with patient movement remain to be addressed. Study of these issues is underway in a rodent survival model.

To date, our experimentation with this novel implantable probe has focused solely on muscle flap monitoring, and our conclusions should not be generalized beyond this. Future studies will assess the potential for this device to monitor buried and difficult-to-access fasciocutaneous flaps, and muscle perfusion in the setting of compartment syndrome.

Conclusion

We have introduced the first NIRS probe which allows continuous monitoring of local StO₂ directly within the substance of muscle tissue. This probe is inexpensive, flexible, subcentimeter in scale, waterproof, biocompatible, and is fitted with resorbable barbs which facilitate temporary autostabilization followed by easy removal. This intramuscular NIRS probe was found to perform near-identically to a cutaneous T.Ox probe in a live porcine myocutaneous flap model of flap ischemia and congestion. This experiment demonstrates the potential suitability of this intramuscular NIRS probe for the task of muscle-only free flap monitoring, and the presented device has the potential to improve monitoring options for flaps which do not bear a skin paddle. Testing in the clinical environment is necessary to assess sensitivity/specificity, durability, and reliability.

Financial Disclosure

Funding for this study was received from the Division of Plastic Surgery and the Department of Neurosurgery at Washington University, and from the Query Simpson Institute of Bioelectronics at Northwestern University.

Conflicts of Interest

Dr. Pet, Dr. MacEwan, and Dr. Rogers have a patent "Novel Wireless Probes for Tissue Perfusion Monitoring" pending. Dr. Arafa reports grants from National Institute of Neurological Disorders and Stroke of the National Institutes of Health under award number F31NS115422, during the conduct of the study.

Matthew MacEwan holds an equity position in Acera Surgical, Inc. and OsteoVantage, Inc., is a board member at Acera Surgical, Inc., and has received funding from ConductiveBio, Inc.

Mitchell A. Pet, MD, has received research funding from Checkpoint Inc. Aside from the issues disclosed above, no authors has any actual or potential conflicts of interest related to the study matter.

References

- Chen K-T, Mardini S, Chuang DC-C, et al. Timing of presentation of the first signs of vascular compromise dictates the salvage outcome of free flap transfers. *Plast Reconstr Surg* 2007;120(01):187–195
- Chao AH, Meyerson J, Povoski SP, Kocak E. A review of devices used in the monitoring of microvascular free tissue transfers. *Expert Rev Med Devices* 2013;10(05):649–660
- Rozen WM, Enajat M, Whitaker IS, Lindkvist U, Audolfsson T, Acosta R. Postoperative monitoring of lower limb free flaps with the Cook-Swartz implantable Doppler probe: a clinical trial. *Microsurgery* 2010;30(05):354–360
- Guillemaud JP, Seikaly H, Cote D, Allen H, Harris JR. The implantable Cook-Swartz Doppler probe for postoperative monitoring in head and neck free flap reconstruction. *Arch Otolaryngol Head Neck Surg* 2008;134(07):729–734
- Zhang T, Dyalram-Silverberg D, Bui T, Caccamese JF Jr, Lubek JE. Analysis of an implantable venous anastomotic flow coupler: experience in head and neck free flap reconstruction. *Int J Oral Maxillofac Surg* 2012;41(06):751–755
- Rozen WM, Chubb D, Whitaker IS, Acosta R. The efficacy of postoperative monitoring: a single surgeon comparison of clinical monitoring and the implantable Doppler probe in 547 consecutive free flaps. *Microsurgery* 2010;30(02):105–110
- Berthelot M, Ashcroft J, Boshier P, et al. Use of near-infrared spectroscopy and implantable Doppler for postoperative monitoring of free tissue transfer for breast reconstruction: a systematic review and meta-analysis. *Plast Reconstr Surg Glob Open* 2019;7(10):e2437–e2438
- Paydar KZ, Hansen SL, Chang DS, Hoffman WY, Leon P. Implantable venous Doppler monitoring in head and neck free flap reconstruction increases the salvage rate. *Plast Reconstr Surg* 2010;125(04):1129–1134
- Kagaya Y, Miyamoto S. A systematic review of near-infrared spectroscopy in flap monitoring: current basic and clinical evidence and prospects. *J Plast Reconstr Aesthet Surg* 2018;71(02):246–257
- Rosenberg JJ, Fornage BD, Chevray PM. Monitoring buried free flaps: limitations of the implantable Doppler and use of color duplex sonography as a confirmatory test. *Plast Reconstr Surg* 2006;118(01):109–113, discussion 114–115
- Ferguson REH Jr, Yu P. Techniques of monitoring buried fasciocutaneous free flaps. *Plast Reconstr Surg* 2009;123(02):525–532
- Keller A. A new diagnostic algorithm for early prediction of vascular compromise in 208 microsurgical flaps using tissue oxygen saturation measurements. *Ann Plast Surg* 2009;62(05):538–543
- Koolen PGL, Vargas CR, Ho OA, et al. Does increased experience with tissue oximetry monitoring in microsurgical breast reconstruction lead to decreased flap loss? The learning effect. *Plast Reconstr Surg* 2016;137(04):1093–1101
- Bai W, Yang H, Ma Y, et al. Flexible transient optical waveguides and surface-wave biosensors constructed from monocrystalline silicon. *Adv Mater* 2018;30(32):e1801584
- Bai W, Shin J, Fu R, et al. Bioresorbable photonic devices for the spectroscopic characterization of physiological status and neural activity. *Nat Biomed Eng* 2019;3(08):644–654
- Bodin F, Diana M, Koutsomanis A, Robert E, Marescaux J, Bruant-Rodier C. Porcine model for free-flap breast reconstruction training. *J Plast Reconstr Aesthet Surg* 2015;68(10):1402–1409
- Baker WB, Parthasarathy AB, Busch DR, Mesquita RC, Greenberg JH, Yodh AG. Modified Beer-Lambert law for blood flow. *Biomed Opt Express* 2014;5(11):4053–4075
- Sassaroli A, Fantini S. Comment on the modified Beer-Lambert law for scattering media. *Phys Med Biol* 2004;49(14):N255–N257
- Kocsis L, Herman P, Eke A. The modified Beer-Lambert law revisited. *Phys Med Biol* 2006;51(05):N91–N98